Matrix Infrared Spectroscopic and Theoretical Studies on the Reactions of Early Lanthanoid Atoms with Nitrous Oxide in Excess Argon

Ling Jiang and Qiang Xu*

National Institute of Advanced Industrial Science and Technology (AIST), Ikeda, Osaka 563-8577, Japan

Received: May 15, 2008; Revised Manuscript Received: June 23, 2008

Reactions of laser-ablated early lanthanoid atoms (Ce, Pr, Nd, Sm, and Eu, except for radioactive Pm) with N_2O molecules in excess argon have been investigated using matrix-isolation infrared spectroscopy. Lanthanoid monoxide−dinitrogen complexes, $OLn(N_2)$ (Ln = Ce, Pr, Nd, and Sm), are observed during sample deposition and identified on the basis of isotopic shifts, mixed isotopic splitting patterns, and CCl_4-doping experiments, whereas no new product is observed for Eu. The $OLnNN^+$ (Ln = Ce, Pr, Nd, and Sm) cations appear during sample deposition and increase visibly upon broadband irradiation ($\lambda > 250$ nm) at the expense of the neutral $OLn(N_2)$ complexes. Density functional theory calculations have been performed on the new products, which support identification of the $OLn(N_2)$ and $OLnNN^+$ complexes from the matrix infrared spectra.

Introduction

Reactions of lanthanoid (Ln) atoms with small molecules (i.e., CO, N_2O, N_2, O_2, NO, H_2, H_2O, CO_2, etc.) have aroused considerable interest both in gas-phase and matrix studies because these reactions have led to a remarkable number of fundamental complexes that provide insight into the lanthanoid chemistry.[1−3] Reactions under nontraditional experimental conditions can often yield exotic species not accessible from high-temperature typical traditional techniques.[4] Recent studies have shown that with the aid of the isotopic substitution technique, matrix-isolation infrared spectroscopy combined with quantum chemical calculation is very powerful in investigating the spectrum, structure, and bonding of novel species.[5,6] For instance, several binary lanthanide metal carbonyls, $Ln(CO)_x$ ($x = 1−6$), have been captured in argon matrix.[1,7] Interestingly, reactions of lanthanide dimers with CO generate a new series of the $Ln_2[\eta^2(\mu_2\text{-C,O})]$ complexes with asymmetrically bridging and side-on-bonded CO ligands, which are drastically activated with remarkably low C−O stretching frequencies.[7d−g]

Previous matrix investigations of the reactions of lanthanoid atoms with N_2 molecules have identified a series of nitride and dinitrogen complexes, LnN, $(LnN)_2$, $Ln(N_2)$, Ln(NN), and $Ln(NN)_2$, revealing that the later lanthanoid metals are less prone to dinitrogen complexation and the nitrides of the later lanthanoid metals require fewer dinitrogen units to achieve saturation.[8] In particular, the Gd_2 dimer reacts with N_2 in solid argon to form a homoleptic dinuclear dinitrogen complex $[Gd_2(\mu\text{-}\eta^2\text{:}\eta^1\text{-}N_2)]$ containing a drastically activated side-on- and end-on-bonded N_2 ligand.[3] This complex rearranges to a planar cyclic $[Gd(\mu\text{-}N)_2Gd]$ isomer with a completely cleaved N−N bond and further dimerizes to form a unique cubic (Gd_4N_4) cluster.[3] Similarly, lanthanoid oxides, hydride, inserted NLnO, $Ln(H_2O)_{1,2}$, and $HLn(OH)_{1,2}$ complexes have been observed and characterized from reactions of lanthanoid atoms with O_2,[9] H_2,[10] NO,[11] and H_2O,[12] respectively.

We recently prepared a series of lanthanoid oxocarbonyl complexes by reactions of lanthanoid atoms with CO_2 in excess argon, revealing intriguing structural and bonding trends in lanthanoid−ligand interactions.[13] It has been demonstrated that the early lanthanoid (La−Sm) oxocarbonyl complexes adopt the trans configurations, the europium and ytterbium ones adopt side-on-bonded modes (Eu−(η^2-OC)O and Yb−(η^2-OC)O), and the late lanthanoid (Gd−Lu) ones adopt the cis configurations, exhibiting the difference in chemistry among the lanthanoid elements.[13] N_2O is isoelectronic with CO_2 but exhibits a global warming potential about 310 times that of CO_2 on a per molecule basis.[14] Gas-phase studies revealed that the reaction of lanthanoid atoms with N_2O leads to N−O bond activation to form LnO and N_2.[2] Here, we report a study of the reactions of early lanthanoid atoms (Ce, Pr, Nd, Sm, and Eu, except for radioactive Pm) with nitrous oxide in excess argon. Infrared spectroscopy coupled with theoretical calculations provides evidence for formation of the metal monoxide−dinitrogen complexes, $OLn(N_2)$, and the $OLnNN^+$ (Ln = Ce, Pr, Nd, and Sm) cation complexes.

Experimental and Theoretical Methods

Experiments for laser ablation and matrix-isolation infrared spectroscopy are similar to those previously reported.[15] In short, the Nd:YAG laser fundamental (1064 nm, 10 Hz repetition rate with 10 ns pulse width) was focused on the rotating early lanthanoid (Ce, Pr, Nd, Sm, and Eu, except for radioactive Pm; 99.9%, Kojundo Chemical Laboratory Co.) targets. The laser-ablated lanthanoid atoms were codeposited with N_2O in excess argon onto a CsI window cooled normally to 4 K by means of a closed-cycle helium refrigerator. Typically, a 1−20 mJ/pulse laser power was used. N_2O (99.5%, Taiyo Nippon Sanso Co.), $^{15}N_2O$ (98%, Cambridge Isotopic Laboratories), and $^{14}N_2O + {}^{15}N_2O$ mixtures were used in different experiments. In general, matrix samples were deposited for 30−60 min with a typical rate of 2−4 mmol/h. After sample deposition, IR spectra were recorded on a BIO-RAD FTS-6000e spectrometer at 0.5 cm^{-1} resolution using a liquid nitrogen cooled HgCdTe (MCT) detector for the spectral range of 5000−400 cm^{-1}. Samples were annealed at different temperatures and subjected to broadband irradiation ($\lambda > 250$ nm) using a high-pressure mercury arc lamp (Ushio, 100 W).

Density functional theory (DFT) calculations were performed to predict the structures and vibrational frequencies of the

* To whom correspondence should be addressed. E-mail: q.xu@aist.go.jp.

10.1021/jp804326g CCC: $40.75
Published on Web 08/21/2008

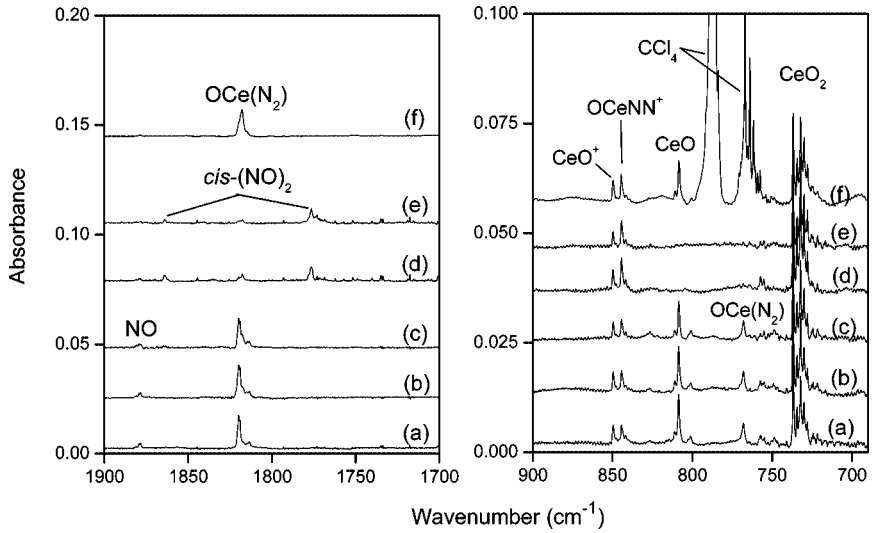

Figure 1. Infrared spectra in the 1900−1700 and 900−700 cm^{-1} regions from codeposition of laser-ablated Ce atoms with 0.4% N_2O in Ar at 4 K: (a) spectrum obtained from initial deposited sample for 1 h, (b) spectrum after annealing to 25 K, (c) spectrum after annealing to 30 K, (d) spectrum after 10 min of broadband irradiation, (e) spectrum after annealing to 35 K, and (f) spectrum obtained by depositing laser-ablated Ce atoms with 0.4% N_2O + 0.03% CCl_4 in Ar at 4 K for 1 h and annealing to 30 K.

observed reaction products using the Gaussian 03 program.[16] All of the present computations employed the BP86 density functional method, but comparisons were done with the B3LYP density functional method as well.[17] The 6-311+G(d) and aug-cc-pVTZ basis sets were used for the N and O atoms,[18] and the scalar-relativistic SDD pseudopotential and basis set were used for the lanthanoid atoms.[19] Geometries were fully optimized, and vibrational frequencies were calculated with analytical second derivatives. Recent investigations have shown that such computational methods can provide reliable information for metal complexes, such as infrared frequencies, relative absorption intensities, and isotopic shifts.[12,20−23]

Results and Discussion

Experiments have been done with N_2O concentrations ranging from 0.05% to 1.0% in excess argon. New species are observed for Ce, Pr, Nd, and Sm but not for Eu. Typical infrared spectra for the reactions of laser-ablated Ce, Pr, Nd, and Sm atoms with N_2O molecules in excess argon in the selected regions are illustrated in Figures 1−8, and the absorption bands in different isotopic experiments are listed in Table 1. The stepwise annealing and irradiation behavior of the product absorptions is also shown in the figures and will be discussed below. Experiments were also done with different concentrations of CCl_4 serving as an electron scavenger.[22]

Quantum chemical calculations have been carried out for the possible isomers and electronic states of the species involved in the Ln + N_2O reactions. DFT calculations show that the optimized structures of the isomers for Ce to Sm are similar to those for Sc, Y, and La.[20,21] Therefore, only the calculated results of the observed products are presented for discussion. The results of the observed and calculated IR frequencies and isotopic frequency ratios for the N−O and Ln−O stretching modes of the products are summarized in Table 2. It has been found that the BP86/6-311+G(d)-SDD (BP86-I) and BP86/aug-cc-pVTZ-SDD (BP86-II) calculations yield essentially similar results (i.e., electronic states, point groups, geometrical parameters, vibrational frequencies, and their intensities); furthermore, the BP86 functional gives calculated vibrational frequencies much closer to the experimental values than the B3LYP functional, as found in many cases such as for the metal complexes.[22,23] Representatively, the N−O and Ln−O stretching vibrational frequencies calculated at the BP86-II level of theory are only given for the Ce system in Table 2. Hereafter, mainly BP86-I results are presented for discussion. The ground electronic states, point groups, vibrational frequencies, and intensities of the products are listed in Table 3. Figure 9 shows the optimized structures of the products.

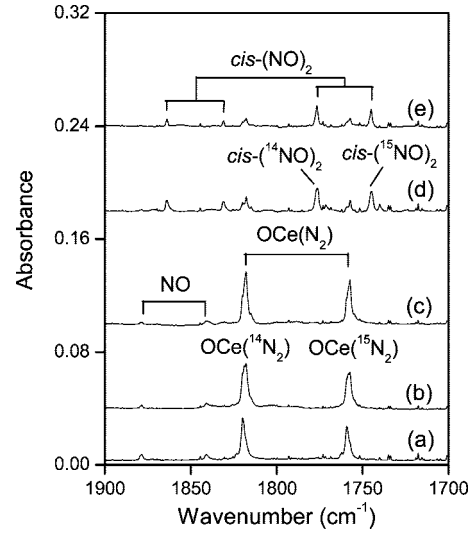

Figure 2. Infrared spectra in the 1900−1700 cm^{-1} region from codeposition of laser-ablated Ce atoms with 0.2% $^{14}N_2O$ + 0.2% $^{15}N_2O$ in Ar at 4 K. For the meaning of a−e, see Figure 1.

A. OLn(N_2) (Ln = Ce, Pr, Nd, Sm). Taking the Ce reaction as an example, two absorptions at 1819.9 and 768.0 cm^{-1} appear together during sample deposition, change little after sample annealing, decrease sharply upon broadband irradiation, and do not reappear after further annealing to higher temperature (Table 1 and Figure 1). The upper band at 1819.9 cm^{-1} shifts to 1759.4 cm^{-1} with $^{15}N_2O$, exhibiting an isotopic frequency ratio ($^{14}N_2O$/$^{15}N_2O$, 1.0344) characteristic of a N−N stretching vibration. The mixed $^{14}N_2O$ + $^{15}N_2O$ isotopic spectra (Figure 2) only provide the sum of pure isotopic bands, which indicates only one N_2 unit is involved in the complex.[25] The 768.0 cm^{-1} band, which is in the spectral range expected for the terminal Ce−O stretching mode,[9a] shows no nitrogen isotopic shift. Furthermore,

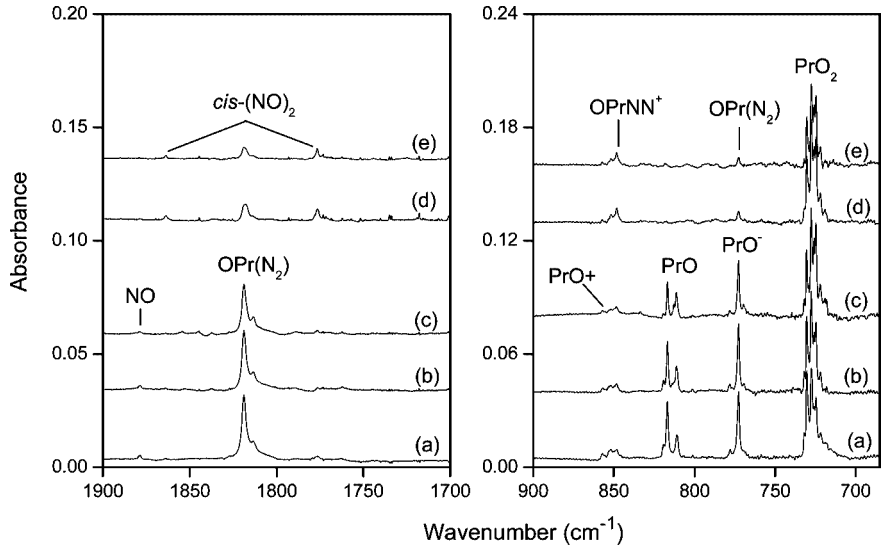

Figure 3. Infrared spectra in the 1900−1700 and 900−700 cm^{-1} regions from codeposition of laser-ablated Pr atoms with 0.3% N_2O in Ar at 4 K. For the meaning of a-e, see Figure 1.

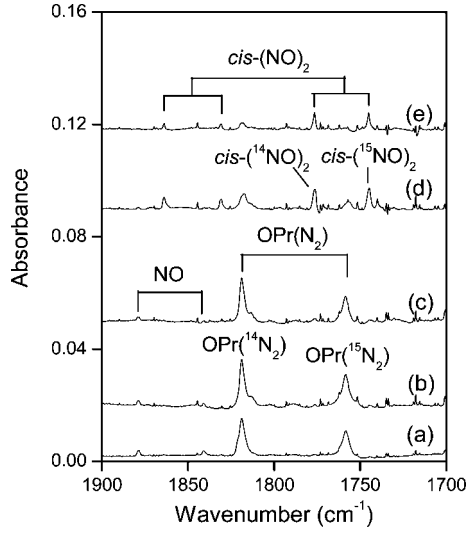

Figure 4. Infrared spectra in the 1900−1700 cm^{-1} region from codeposition of laser-ablated Pr atoms with 0.2% $^{14}N_2O$ + 0.2% $^{15}N_2O$ in Ar at 4 K. For the meaning of a−e, see Figure 1.

doping with CCl_4 has no effect on these bands (Figure 1, trace f), suggesting that the products are neutral.[22] The features of the IR spectra in the present matrix experiments are reminiscent of those of the side-bonded structure of $OLa(N_2)$ in which the corresponding N−N stretching vibrational frequencies appear at 1811.6 and 759.4 cm^{-1} in the argon matrix experiments.[21] Accordingly, the 1819.9 and 768.0 cm^{-1} bands are assigned to the N−N and Ce−O stretching vibrations of the neutral $OCe(N_2)$ complex on the basis of the results of the isotopic substitution, N_2O concentration change, and CCl_4-doping experiments. The Ce−O stretching vibration of $OCe(N_2)$ (768.0 cm^{-1}) is 40.3 cm^{-1} red shifted from the corresponding IR absorption of CeO (808.3 cm^{-1}).[9a] The N−N and M−O stretching vibrations of $OM(N_2)$ appear at 1817.2 and 906.5 cm^{-1} for M = Sc and 1809.8 and 802.3 cm^{-1} for M = Y, respectively, in the argon matrix.[20]

DFT calculations predict the $OCe(N_2)$ complex to have a $^3A'$ ground-state with C_s symmetry (Table 3 and Figure 9). The Ce−O, Ce−N, and N−N distances are calculated to be 1.832, 2.530, and 1.173 Å (Figure 9), respectively. The N−N and Ce−O stretching vibrational frequencies are calculated to be 1840.7 and 772.5 cm^{-1} (Table 3, BP86-I level), which should be multiplied by 0.989 and 0.994 to fit the experimental values of 1819.9 and 768.0 cm^{-1}, respectively, showing good scale factors.[26] As listed in Table 2, the calculated $^{14}N_2O/^{15}N_2O$ isotopic frequency ratios for the N−N and Ce−O stretching vibrations are consistent with experimental values. These agreements between the experimental and calculated vibrational frequencies, relative absorption intensities, and isotopic shifts confirm the identification of the $OCe(N_2)$ complex from the matrix IR spectra.

TABLE 1: IR Absorptions (in cm^{-1}) Observed from Co-Deposition of Laser-Ablated Ce, Pr, Nd, and Sm Atoms with N_2O in Excess Argon at 4 K

$^{14}N_2O$	$^{15}N_2O$	$^{14}N_2O$ + $^{15}N_2O$	$^{14}N_2O/^{15}N_2O$	assignment
1819.9	1759.4	1819.9, 1759.4	1.0344	$OCe(N_2)$
844.4	844.4		1.0000	$OCeNN^+$
768.0	768.0		1.0000	$OCe(N_2)$
1818.8	1758.4	1818.8, 1758.4	1.0343	$OPr(N_2)$
848.2	848.2		1.0000	$OPrNN^+$
772.6	772.6		1.0000	$OPr(N_2)$
1821.5	1761.0	1821.5, 1761.0	1.0344	$ONd(N_2)$
844.3	844.3		1.0000	$ONdNN^+$
771.6	771.6		1.0000	$ONd(N_2)$
1813.3	1754.0	1813.3, 1754.0	1.0338	$OSm(N_2)$
835.3	835.3		1.0000	$OSmNN^+$
760.8	760.8		1.0000	$OSm(N_2)$

In the reactions of N_2O with Pr, Nd, and Sm atoms, the absorptions of the analogous $OLn(N_2)$ (Ln = Pr, Nd, and Sm) complexes have been observed in the regions of 1900−1700 and 900−700 cm^{-1} (Pr, 1818.8, 772.6; Nd, 1821.5, 771.6; Sm, 1818.3, 760.8 cm^{-1}) (Table 1 and Figures 3−8), respectively. The calculated N−N stretching frequencies are systematically higher than the observed values (Table 2), which may be caused by the inefficiency of the XC functional and/or the basis sets used here, posing a formidable theoretical challenge because of the large numbers of f electrons and strong relativistic effects.[24] However, the calculated $^{14}N_2O/^{15}N_2O$ isotopic frequency ratios are consistent with the observed values. Furthermore, good agreements between the experimental and calculated vibrational frequencies, relative absorption intensities, and isotopic shifts have also been obtained for the Ln−O stretching vibrations (Tables 2 and 3).

B. $OLnNN^+$ (Ln = Ce, Pr, Nd, Sm). In the reaction of Ce atoms with N_2O in the argon matrix, the absorption at 844.4

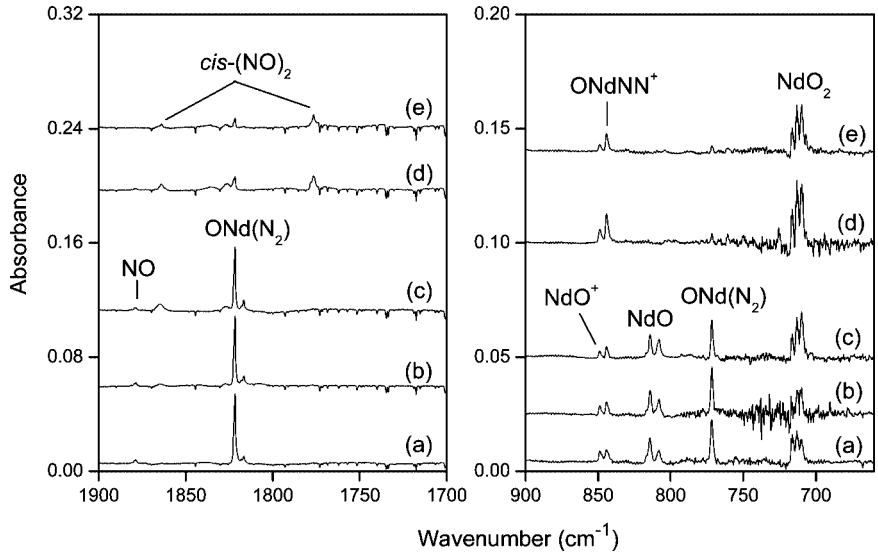

Figure 5. Infrared spectra in the 1900−1700 and 900−700 cm^{-1} regions from codeposition of laser-ablated Nd atoms with 0.3% N_2O in Ar at 4 K. For the meaning of a−e, see Figure 1.

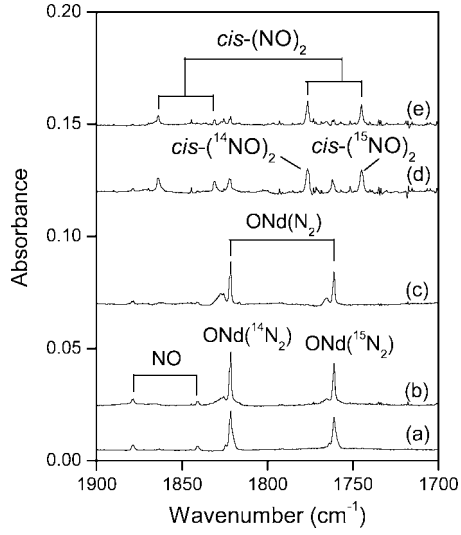

Figure 6. Infrared spectra in the 1900−1700 cm^{-1} region from codeposition of laser-ablated Nd atoms with 0.2% $^{14}N_2O$ + 0.2% $^{15}N_2O$ in Ar at 4 K. For the meaning of a−e, see Figure 1.

cm^{-1} appears during sample deposition, changes little after annealing, and increases markedly upon broadband irradiation at the expense of the neutral $OCe(N_2)$ complex (Table 1 and Figure 1), indicating that this new species also has the CeN_2O stiochiometry. The band at 844.4 cm^{-1}, which is in the spectral range expected for the terminal Ce−O stretching mode,[9a] shows no nitrogen isotopic shift. Doping with CCl_4 visibly increases this band (Figure 1, trace f), suggesting that the product is cationic.[22] Although the 844.4 cm^{-1} band is only 5.0 cm^{-1} red shifted from the Ce−O stretching vibration of the CeO^+ cation (849.4 cm^{-1}),[9a] the behavior of sample annealing and irradiation for the 844.4 cm^{-1} band is different from that for the 849.4 cm^{-1} band of the CeO^+ cation (Figure 1). By analogy with the $OMNN^+$ (M = Sc, Y, and La) spectra,[20,21] the 844.4 cm^{-1} band is assigned to the Ce−O stretching mode of the $OCeNN^+$ cation.

BP86 calculations show that the $OCeNN^+$ complex has a $^2A''$ ground-state with C_s symmetry (Table 3 and Figure 9). The calculated Ce−O stretching mode is 882.2 cm^{-1} (Tables 2 and 3), which should be multiplied by 0.957 to fit the observed value of 844.4 cm^{-1}, giving a reasonable scale factor.[26] The N−N

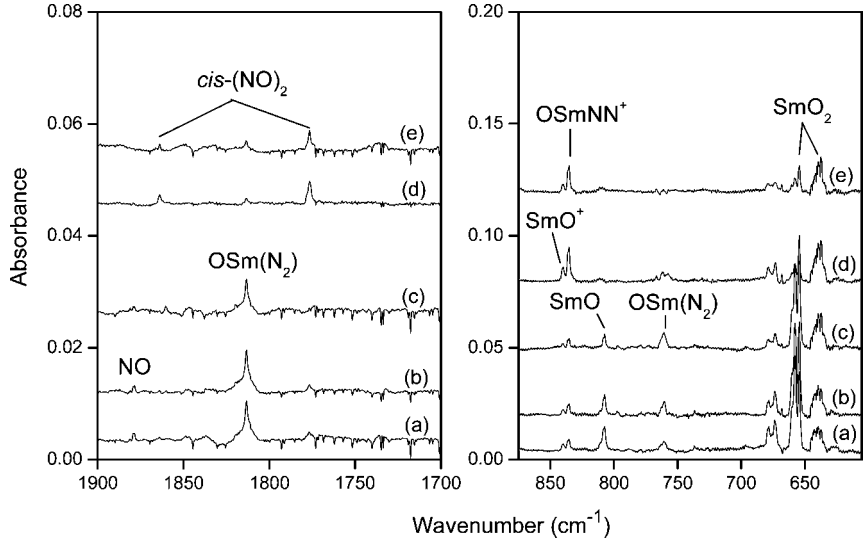

Figure 7. Infrared spectra in the 1900−1700 and 850−650 cm^{-1} regions from codeposition of laser-ablated Sm atoms with 0.3% N_2O in Ar at 4 K. For the meaning of a−e, see Figure 1.

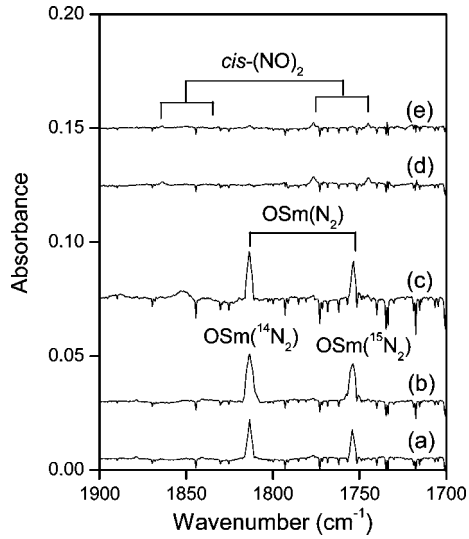

Figure 8. Infrared spectra in the 1900−1700 cm^{-1} region from codeposition of laser-ablated Sm atoms with 0.2% $^{14}N_2O$ + 0.2% $^{15}N_2O$ in Ar at 4 K. For the meaning of a−e, see Figure 1.

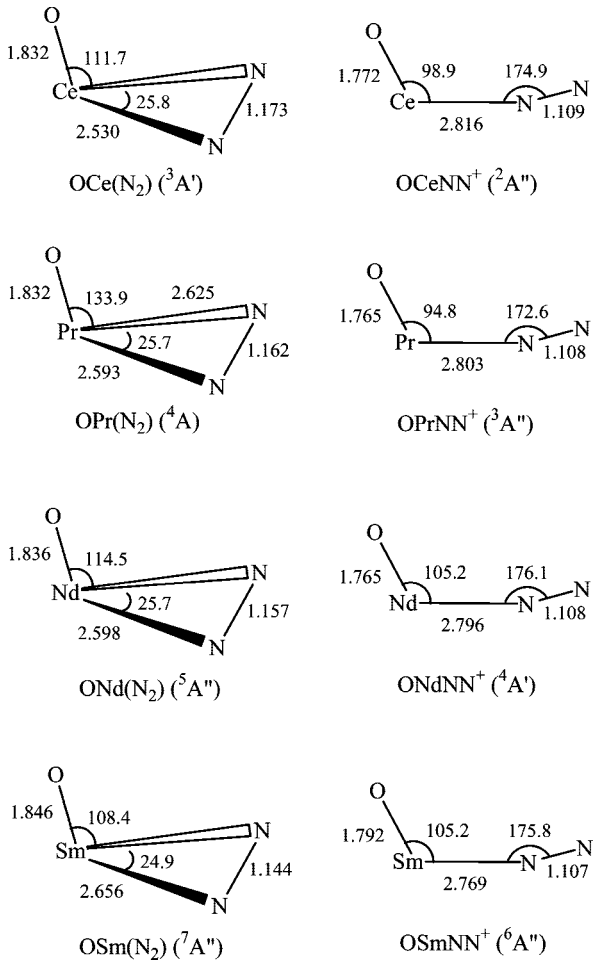

Figure 9. Optimized structures (bond lengths in angstroms, bond angles in degrees) of the products calculated at the BP86/6-311+G(d)-SDD level.

stretching vibration is predicted to be 2315.3 cm^{-1}. With its small intensity (18 km/mol) it is not likely to be observed, which is consistent with the absence from the present experiments.

The Pr, Nd, and Sm experiments produce the absorptions of the analogous $OLnNN^+$ (Ln = Pr, Nd, and Sm) complexes at

TABLE 2: Comparison of Observed and Calculated IR Frequencies (in cm^{-1}) and Isotopic Frequency Ratios for the Products

		observed		calculated		
species	mode	freq	$^{14}N_2O/^{15}N_2O$	method	freq	$^{14}N_2O/^{15}N_2O$
$OCe(N_2)$	ν_{N-N}	1819.9	1.0344	BP86-I[a]	1840.7	1.0350
				BP86-II[b]	1843.8	1.0350
				B3LYP[a]	1938.4	1.0350
	ν_{Ce-O}	768.0	1.0000	BP86-I	772.5	1.0000
				BP86-II	771.2	1.0000
				B3LYP	794.0	1.0000
$OPr(N_2)$	ν_{N-N}	1818.8	1.0343	BP86-I	1904.8	1.0348
				B3LYP	1937.0	1.0348
	ν_{Pr-O}	772.6	1.0000	BP86-I	760.1	1.0000
				B3LYP	793.7	1.0000
$ONd(N_2)$	ν_{N-N}	1821.5	1.0344	BP86-I	1948.8	1.0349
				B3LYP	1946.9	1.0349
	ν_{Nd-O}	771.6	1.0000	BP86-I	752.6	1.0000
				B3LYP	785.6	1.0000
$OSm(N_2)$	ν_{N-N}	1818.3	1.0338	BP86-I	2025.4	1.0350
				B3LYP	2121.8	1.0350
	ν_{Sm-O}	760.8	1.0000	BP86-I	744.0	1.0000
				B3LYP	775.1	1.0000
$OCeNN^+$	ν_{Ce-O}	844.4	1.0000	BP86-I	882.2	1.0000
				BP86-II	882.5	1.0000
				B3LYP	905.0	1.0000
$OPrNN^+$	ν_{Pr-O}	848.2	1.0000	BP86-I	882.9	1.0000
				B3LYP	912.8	1.0000
$ONdNN^+$	ν_{Nd-O}	844.3	1.0000	BP86-I	860.8	1.0000
				B3LYP	902.7	1.0000
$OSmNN^+$	ν_{Sm-O}	835.3	1.0000	BP86-I	742.8	1.0000
				B3LYP	856.5	1.0000

[a] 6-311+G(d) basis set on N and O atoms. [b] Aug-cc-pVTZ basis set on N and O atoms.

848.2, 844.3, and 835.3 cm^{-1} (Table 1 and Figures 3, 5, and 7), respectively. BP86 calculations predict the $OLnNN^+$ (Ln = Pr, Nd, and Sm) complexes to have $^3A''$, $^4A'$, and $^6A''$ ground states with C_s symmetries (Figure 9), respectively. It can be seen from Figure 9 that the Ln−O and N−N distances in the $OLnNN^+$ (Ln = Ce, Pr, Nd, and Sm) complexes are slightly shorter than those in the $OLn(N_2)$ complexes, whereas the Ln−N distances in the $OLnNN^+$ complexes are longer than those in the $OLn(N_2)$ complexes. The calculated Ln−O stretching modes are 882.9, 860.8, and 742.8 cm^{-1} (Tables 2 and 3), which are in agreement with experimental values of 848.2, 844.3, and 835.3 cm^{-1}, respectively.

C. Reaction Mechanism. On the basis of the behavior of sample annealing and irradiation, together with the observed species and calculated stable isomers, a plausible reaction mechanism can be proposed as follows. Under the present experimental conditions, the $OLn(N_2)$ (Ln = Ce, Pr, Nd, and Sm) complexes are the primary products during sample deposition (Figures 1, 3, 5, and 7), suggesting that spontaneous insertion of laser-ablated Ce, Pr, Nd, and Sm atoms into N_2O to form these side-bonded complexes is the dominant process (reaction 1). Recent studies on the Y and La systems indicated that the reactions start by binding the outer nitrogen atom of N_2O with the metal atom to form a planar intermediate MNNO (M = Y and La) and then rearrange to form a side-bonded intermediate M−(η^2-NN)O and the oxygen atom can further be transferred to form $OM(N_2)$.[21] Similar isomerizations from LnNNO to $OLn(N_2)$ via Ln−(η^2-NN)O for the Ce, Pr, Nd, and Sm reactions have also been obtained, and the details could be referred to the Y and La systems.[21]

TABLE 3: Ground Electronic States, Point Groups, Vibrational Frequencies (in cm^{-1}), and Intensities (km/mol) of the Products Calculated at the BP86/6-311+G(d)-SDD Level

species	elec state	point group	frequency (intensity, mode)
$OCe(N_2)$	$^3A'$	C_s	1840.7 (408, A′), 772.5 (317, A′), 254.1 (1, A′), 241.0 (15, A″), 101.8 (4, A″), 101.1 (19, A′)
$OCeNN^+$	$^2A''$	C_s	2315.3 (18, A′), 882.2 (188, A′), 167.4 (1, A′), 152.7 (1, A″), 128.2 (2, A′), 8.1 (21, A′)
$OPr(N_2)$	^4A	C_1	1904.8 (487, A), 760.1 (363, A), 303.6 (7, A), 235.4 (5, A), 135.8 (20, A), 111.6 (10, A)
$OPrNN^+$	$^3A''$	C_s	2337.2 (3, A′), 882.9 (166, A′), 174.0 (3, A′), 153.7 (1, A″), 138.8 (9, A′), 90.7 (16, A′)
$ONd(N_2)$	$^5A''$	C_s	1948.8 (311, A′), 752.6 (332, A′), 344.3 (5, A″), 259.7 (18, A′), 116.6 (9, A″), 91.9 (11, A′)
$ONdNN^+$	$^4A'$	C_s	2340.4 (8, A′), 860.8 (164, A′), 176.5 (3, A′), 155.4 (1, A″), 138.4 (8, A′), 69.2 (17, A′)
$OSm(N_2)$	$^7A''$	C_s	2025.4 (429, A′), 744.0 (266, A′), 196.4 (1, A′), 135.9 (3, A″), 106.5 (24, A′), 99.5 (5, A″)
$OSmNN^+$	$^6A''$	C_s	2345.1 (15, A′), 742.8 (102, A′), 158.3 (1, A′), 152.2 (1, A″), 142.8 (9, A′), 44.9 (22, A′)

$$Ln + N_2O \rightarrow OLn(N_2) \quad (Ln = Ce, Pr, Nd, \text{and } Sm) \quad (1)$$

Recent investigations have shown that laser ablation of metal targets produces not only neutral metal atoms but also metal cations and electrons. Ionic metal complexes can also be formed in the reactions with small molecules.[22] In the present experiments, $OLnNN^+$ cations appear during sample deposition and increase markedly upon broadband irradiation at the expense of the neutral $OLn(N_2)$ complexes (Figures 1, 3, 5, and 7), suggesting that the $OLnNN^+$ cations may be generated by photoionization of the neutral $OLn(N_2)$ complexes via radiation in the ablation plume and/or broadband irradiation (reaction 2). The ionization energies of $OLn(N_2)$ (Ln = Ce, Pr, Nd, and Sm) are calculated to be 128.1, 128.6, 131.1, and 146.3 kcal/mol, respectively, which exceed the mercury arc energy (115 kcal/mol at 250 nm). This suggests that an $OLn(N_2)^*$ excited state is sufficiently long lived to absorb a second photon to reach ionization. Furthermore, the NNO_2^- anion absorptions also increased on broadband irradiation, which serves as a counterion to preserve the matrix electric neutrality. Similar results have also been found for group 3 metal atoms.[20,21]

$$OLn(N_2) - e^- \rightarrow OLnNN^+ \quad (2)$$

It is noted that the N−N stretching vibrations of the neutral $OLn(N_2)$ (Ce, 1819.9; Pr, 1818.8; Nd, 1821.5; Sm, 1818.3 cm^{-1}) complexes are quite close to those of $OM(N_2)$ (Sc, 1817.2; Y, 1809.8; La, 1811.6 cm^{-1}),[20,21] suggesting the reactivity of N_2O toward the early lanthanoid atoms is similar to the reactivity of N_2O toward group 3 metal atoms.

Conclusions

This paper reports a systematic study on the reactions of early lanthanoids (Ce, Pr, Nd, Sm, and Eu, except for radioactive Pm) with N_2O molecules using matrix-isolation infrared spectroscopy. On the basis of the results of the isotopic substitution, N_2O concentration change, and CCl_4-doping experiments, the $OLn(N_2)$ and $OLnNN^+$ (Ln = Ce, Pr, Nd, and Sm) complexes have been isolated and characterized in argon matrix, whereas no such species is apparent with Eu. Density functional theory calculations have been performed on the products. The agreement between the experimental and calculated vibrational frequencies, relative absorption intensities, and isotopic shifts supports identification of new species from the matrix infrared spectra. The present investigations show that the N−N stretching vibrations of $OLn(N_2)$ (Ce, 1819.9; Pr, 1818.8; Nd, 1821.5; Sm, 1818.3 cm^{-1}) complexes are quite close to those of $OM(N_2)$ (Sc, 1817.2; Y, 1809.8; La, 1811.6 cm^{-1}).

Acknowledgment. The authors would like to express thanks to the reviewers for valuable suggestions. This work was supported by AIST and a Grant-in-Aid for Scientific Research (B) (Grant No. 17350012) from the Ministry of Education, Culture, Sports, Science and Technology (MEXT) of Japan. L.J. is grateful to the Japan Society for Promotion of Science (JSPS) for a postdoctoral fellowship.

References and Notes

(1) (a) Sheline, R. K.; Slater, J. L. *Angew. Chem., Int. Ed.* **1975**, *14*, 309. (b) Gottfriedsen, J.; Edelmann, F. T. *Coord. Chem. Rev.* **2007**, *251*, 142.

(2) Campbell, M. L. *J. Chem. Phys.* **1999**, *111*, 562.

(3) Zhou, M. F.; Jin, X.; Gong, Y.; Li, J. *Angew. Chem., Int. Ed.* **2007**, *46*, 2911.

(4) (a) For example, see: Bandy, R. E.; Lakshminarayan, C.; Frost, R. K.; Zwier, T. S. *J. Chem. Phys.* **1993**, *98*, 5362. (b) Wang, L. S.; Cheng, H. S.; Fan, J. *J. Chem. Phys.* **1995**, *102*, 9840. (c) Duncan, M. A. *Int. Rev. Phys. Chem.* **2003**, *22*, 407.

(5) (a) For example, see: Xu, C.; Manceron, L.; Perchard, J. P. *J. Chem. Soc., Faraday Trans.* **1993**, *89*, 1291. (b) Bondybey, V. E.; Smith, A. M.; Agreiter, J. *Chem. Rev.* **1996**, *96*, 2113. (c) Fedrigo, S.; Haslett, T. L.; Moskovits, M. *J. Am. Chem. Soc.* **1996**, *118*, 5083. (d) Khriachtchev, L.; Pettersson, M.; Runeberg, N.; Lundell, J.; Rasanen, M. *Nature* **2000**, *406*, 874. (e) Himmel, H. J.; Manceron, L.; Downs, A. J.; Pullumbi, P. *J. Am. Chem. Soc.* **2002**, *124*, 4448. (f) Li, J.; Bursten, B. E.; Liang, B.; Andrews, L. *Science* **2002**, *295*, 2242. (g) Andrews, L.; Wang, X. *Science* **2003**, *299*, 2049.

(6) (a) Zhou, M. F.; Tsumori, N.; Li, Z.; Fan, K.; Andrews, L.; Xu, Q. *J. Am. Chem. Soc.* **2002**, *124*, 12936. (b) Zhou, M. F.; Xu, Q.; Wang, Z.; Schleyer, P. v. R. *J. Am. Chem. Soc.* **2002**, *124*, 14854. (c) Jiang, L.; Xu, Q. *J. Am. Chem. Soc.* **2005**, *127*, 42. (d) Xu, Q.; Jiang, L.; Tsumori, N. *Angew. Chem., Int. Ed.* **2005**, *44*, 4338. (e) Jiang, L.; Xu, Q. *J. Am. Chem. Soc.* **2005**, *127*, 8906. (f) Jiang, L.; Xu, Q. *J. Am. Chem. Soc.* **2006**, *128*, 1394.

(7) (a) Slater, J. L.; Sheline, R. K.; Lin, K. C.; Weltner, W., Jr *J. Chem. Phys.* **1971**, *55*, 5129. (b) Slater, J. L.; DeVore, T. C.; Calder, V. *Inorg. Chem.* **1973**, *12*, 1918. (c) Slater, J. L.; DeVore, T. C.; Calder, V. *Inorg. Chem.* **1974**, *13*, 1808. (d) Xu, Q.; Jiang, L.; Zou, R. Q. *Chem. Eur. J.* **2006**, *12*, 3226. (e) Zhou, M. F.; Jin, X.; Li, J. *J. Phys. Chem. A* **2006**, *110*, 10206. (f) Jin, X.; Jiang, L.; Xu, Q.; Zhou, M. F. *J. Phys. Chem. A* **2006**, *110*, 12585. (g) Jiang, L.; Jin, X.; Zhou, M. F.; Xu, Q. *J. Phys. Chem. A* **2008**, *112*, 3627.

(8) (a) Willson, S. P.; Andrews, L. *J. Phys. Chem. A* **1998**, *102*, 10238. (b) Willson, S. P.; Andrews, L. *J. Phys. Chem. A* **1999**, *103*, 1311.

(9) (a) Willson, S. P.; Andrews, L. *J. Phys. Chem. A* **1999**, *103*, 3171. (b) Willson, S. P.; Andrews, L. *J. Phys. Chem. A* **1999**, *103*, 6972.

(10) Willson, S. P.; Andrews, L. *J. Phys. Chem. A* **2000**, *104*, 1640.

(11) Willson, S. P.; Andrews, L.; Neurock, M. *J. Phys. Chem. A* **2000**, *104*, 3446.

(12) (a) Xu, J.; Zhou, M. F. *J. Phys. Chem. A* **2006**, *110*, 10575. (b) Xu, J.; Jin, X.; Zhou, M. F. *J. Phys. Chem. A* **2007**, *111*, 7105.

(13) Jiang, L.; Zhang, X. B.; Han, S.; Xu, Q. *Inorg. Chem.* **2008**, *47*, 4826.

(14) Trogler, W. C. *Coord. Chem. Rev.* **1999**, *187*, 303.

(15) (a) Burkholder, T. R.; Andrews, L. *J. Chem. Phys.* **1991**, *95*, 8697. (b) Zhou, M. F.; Tsumori, N.; Andrews, L.; Xu, Q. *J. Phys. Chem. A* **2003**, *107*, 2458. (c) Jiang, L.; Xu, Q. *J. Chem. Phys.* **2005**, *122*, 034505. (d) Jiang, L.; Teng, Y. L.; Xu, Q. *J. Phys. Chem. A* **2006**, *110*, 7092.

(16) Frisch, M. J.; Trucks, G. W.; Schlegel, H. B.; Scuseria, G. E.; Robb, M. A.; Cheeseman, J. R.; Montgomery, J. A., Jr.; Vreven, T.; Kudin, K. N.; Burant, J. C.; Millam, J. M.; Iyengar, S. S.; Tomasi, J.; Barone, V.; Mennucci, B.; Cossi, M.; Scalmani, G.; Rega, N.; Petersson, G. A.; Nakatsuji, H.; Hada, M.; Ehara, M.; Toyota, K.; Fukuda, R.; Hasegawa, J.; Ishida, M.; Nakajima, T.; Honda, Y.; Kitao, O.; Nakai, H.; Klene, M.; Li, X.; Knox, J. E.; Hratchian, H. P.; Cross, J. B.; Adamo, C.; Jaramillo, J.; Gomperts, R.; Stratmann, R. E.; Yazyev, O.; Austin, A. J.; Cammi, R.; Pomelli, C.; Ochterski, J. W.; Ayala, P. Y.; Morokuma, K.; Voth, G. A.; Salvador, P.; Dannenberg, J. J.; Zakrzewski, V. G.; Dapprich, S.; Daniels, A. D.; Strain, M. C.; Farkas, O.; Malick, D. K.; Rabuck, A. D.; Raghavachari, K.; Foresman, J. B.; Ortiz, J. V.; Cui, Q.; Baboul, A. G.; Clifford, S.; Cioslowski, J.; Stefanov, B. B.; Liu, G.; Liashenko, A.; Piskorz, P.; Komaromi, I.; Martin, R. L.; Fox, D. J.; Keith, T.; Al-Laham, M. A.; Peng, C. Y.; Nanayakkara, A.; Challacombe, M.; Gill, P. M. W.; Johnson, B.; Chen, W.; Wong, M. W.; Gonzalez, C.; Pople, J. A. *Gaussian 03*, revision B.04; Gaussian, Inc.: Pittsburgh, PA, 2003.

(17) (a) Becke, A. D. *Phys. Rev. A* **1988**, *38*, 3098. (b) Perdew, J. P. *Phys. Rev. B* **1986**, *33*, 8822. (c) Lee, C.; Yang, E.; Parr, R. G. *Phys. Rev. B* **1988**, *37*, 785. (d) Becke, A. D. *J. Chem. Phys.* **1993**, *98*, 5648.

(18) (a) McLean, A. D.; Chandler, G. S. *J. Chem. Phys.* **1980**, *72*, 5639. (b) Krishnan, R.; Binkley, J. S.; Seeger, R.; Pople, J. A. *J. Chem. Phys.* **1980**, *72*, 650. (c) Dunning, T. H., Jr *J. Chem. Phys.* **1989**, *90*, 1007. (d) Kendall, R. A.; Dunning, T. H., Jr.; Harrison, R. J. *J. Chem. Phys.* **1992**, *96*, 6796.

(19) Andrae, D.; Haeussermann, U.; Dolg, M.; Stoll, H.; Preuss, H. *Theor. Chim. Acta* **1990**, *77*, 123.

(20) Zhou, M. F.; Wang, G. J.; Zhao, Y. Y.; Chen, M. H.; Ding, C. F. *J. Phys. Chem. A* **2005**, *109*, 5079.

(21) Jiang, L.; Xu, Q. *J. Phys. Chem. A* , ASAP Article, Web Release Date: 21-Jun-2008; DOI: 10.1021/jp802114z (Y, La + N_2O).

(22) (a) Zhou, M. F.; Andrews, L.; Bauschlicher, C. W., Jr *Chem. Rev.* **2001**, *101*, 1931. (b) Andrews, L.; Citra, A. *Chem. Rev.* **2002**, *102*, 885. (c) Himmel, H. J.; Downs, A. J.; Greene, T. M. *Chem. Rev.* **2002**, *102*, 4191.

(23) Jiang, L.; Xu, Q. *J. Chem. Phys.* **2008**, *128*, 124317.

(24) For example, see:(a) Pyykkö, P. *Chem. Rev.* **1988**, *88*, 563. (b) Pepper, M.; Bursten, B. E. *Chem. Rev.* **1991**, *91*, 719. (c) Seth, M.; Dolg, M.; Fulde, P.; Schwerdtfeger, P. *J. Am. Chem. Soc.* **1995**, *117*, 6597. (d) Li, J.; Bursten, B. E. *J. Am. Chem. Soc.* **1997**, *119*, 9021.

(25) Darling, J. H.; Ogden, J. S. *J. Chem. Soc., Dalton Trans.* **1972**, 2496.

(26) Merrick, J. P.; Moran, D.; Radom, L. *J. Phys. Chem. A* **2007**, *111*, 11683.

JP804326G